

# Performance Assessment of Single Stage and Multi-Stage L-WIXCs Considering Coherent and Incoherent Crosstalk

Md Asif Iqbal<sup>1</sup>,

Mohammad Manzoor-E-Elahee<sup>2</sup>, and Satya Prasad Majumder<sup>3</sup>, Non-members

## ABSTRACT

The statistical impact of Coherent and Incoherent Crosstalk Contributions on the performance of a proposed single stage and a multi-stage Share-per-Node  $L - WIXC$  configuration and a multi-stage Share-per-Wavelength  $L - WIXC$  configuration in terms of different Optical Propagation Delay Differences, Bit Duration etc., is compared both theoretically and analytically. Besides, considering Coherent and Incoherent Crosstalk contributions for each of those cases, analytical expressions of Electric Field, Leakage Crosstalk, Bit-Error-Rate ( $BER$ ) and Power Penalty ( $pp$ ) are being developed. Finally, the results obtained numerically, are thoroughly compared on the basis of Optimum Number of Wavelength Converters, Number of Inputs and Number of Wavelengths per Input Channel.

**Keywords:** Coherent Crosstalk, Incoherent Crosstalk,  $L - WIXC$ , Power Penalty, Bit-Error-Rate, Relative Intensity Noise (RIN), Share-per-Wavelength

## 1. INTRODUCTION

Apart from complexity and expense problems, Scalability and Expandability are two important issues of the existing optical networks having limited wavelength conversion capability. Consequently, leading us to the efficient design of the same while ensuring the Optimum Performance and Minimum Cost. Several architectures for Optical-Cross-Connects ( $OXC$ ) were proposed [1-5] with and without wavelength conversion capability. Unlike  $WIXC$ , proposed Limited-Wavelength-Interchange-Cross-Connects ( $L - WIXCs$ ) [5] have limited number of shared converters between inputs and out-

puts. In contrast to that, a new generation of Share-per-Wavelength grouping scheme was proposed [6], where the whole wavelength (including  $SSMs$  were) was equally divided into several groups having same wavelength and wavelength converters ( $WCs$ ) were shared within the group; thereby greatly improving the Blocking Performance, Expandability and Scalability. These particular architectures, which are either Share-per-Node or Share-per-Wavelength, either single stage or multistage, are designed with a view to ensure the optimum use of limited resources and improved  $BER$  performance and Power Penalty [6]. Mentionable that, among various crosstalk components, Coherent and Incoherent Crosstalk is most crucial in analysing a system and evaluate its performance [3]. In this paper, using these architectures, the effect of different wavelength grouping schemes and different crosstalk contributions (e.g. Coherent and Incoherent) on the  $BER$  performance and Power Penalty is studied and compared analytically in terms of different input level and network parameters (e.g. optical propagation delay differences, bit duration, leakage crosstalk etc.) [4]. Finally, the Power Penalty and the total Crosstalk Contributions due to different crosstalk components [7-8] are also derived and evaluated numerically for an optimal value of  $BER$ .

## 2. THE CROSSTALK MODELS

### 2.1 Single Stage $L - WIXC$ , $SSM-1$

A typical single stage Share-Per-Node architecture of  $L - WIXC$  with Partial wavelength converter sharing [5] is shown in Fig. 1

It consists of  $N$  optical De-Multiplexers and Multiplexers, a compact Space Switching Matrix ( $SSM$ ) and a typical  $CxNCSSM$ . Each of the  $M$  light paths from each of the  $N$  De-Multiplexers passes through the first  $SSM$  before they are directed towards the destination Multiplexer. Besides, there are  $C$  converters (shared by each node) which convert the portion of the incoming signal and forward them towards the second  $SSM$  which ultimately routes all the converted signals towards the destination Multiplexer that combines signals from a total of  $(M + C)$  light paths each. Hence, the number of cross-points in this architecture can be written as  $NM(NM + C) + NC^2$ .

Manuscript received on April 10, 2012 ; revised on October 18, 2012.

<sup>1,2</sup> The authors are with Electrical Electronic and Communication Engineering Department, Military Institute of Science and Technology Mirpur Cantonment, Dhaka-1216, Bangladesh., E-mail: asif\_eece\_mist@yahoo.com and manzoor4210@yahoo.com

<sup>3</sup> The author is with Electrical and Electronic Engineering Department, Bangladesh University of Engineering and Technology Dhaka-1000, Bangladesh., E-mail: spmajumder@eee.buet.ac.bd

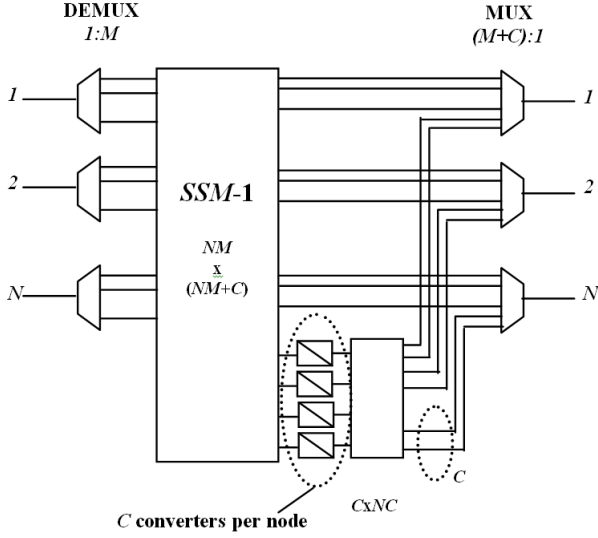


**Fig.1:** A Single Stage Share-Per-Node Architecture of L-WIXC SSM (SSM-1).

## 2.2 Multi-Stage L – WIXC, SSM-2

In practice, the switching function of an OXC is often implemented in multiple stages in order to reduce its overall complexity. *SSM-2*, as depicted in Fig. 2, is a multi-stage realization of *SSM-1* with strict full sharing of wavelength converters. This *L – WIXC* requires  $MNx(N+1)$  *SSMs*, one  $MxCSSM$ , one  $CxNC$  *SSM* and  $NM$  Tunable Filters. Each of the  $M$  paths passes through a *SSM* before they are combined with the outputs from the other  $(M-1)$  *SSMs*. Besides, there are  $C$  converters (shared by each node) which convert the portion of the incoming signal and forward them towards the second *SSM* which ultimately routes all the converted signals towards the destination Multiplexer that combines signals from a total of  $(M+C)$  light paths each. The number of *SSMs*, which is required to achieve strictly non-blocking behavior and strict full converter sharing would be at least  $M+C-1$ . The *SSMs* will have a total of  $NM(N+1) + MC + NC^2$  cross-points.

## 2.3 Grouped L – WIXC, SSM-3

A typical multistage and grouped Share-Per-Wavelength architecture of *L – WIXC* with *Re-arrangeable Full* wavelength converter sharing [5] is shown in Fig. 3. Let,  $M$  denote the number of the wavelength in an OXC, and  $N$  is the number of WCs for a wavelength *SSM* as described above.  $S_G$  is the size of wavelength-group and  $G$  is the number of groups; assuming that every group has the same size. Within a group, the  $S_G$  wavelengths are connected in the rule same as that in no grouping structure. The  $i^{th}$  wavelength in the group is converted to  $(i+l)^{th}$  ( $1 < l < N, i+l \leq S_G$ ) and  $(i+l-S_G)^{th}$  ( $1 < l < N, i+l > S_G$ ) wavelength in the group. When the OXC is to be expanded for the

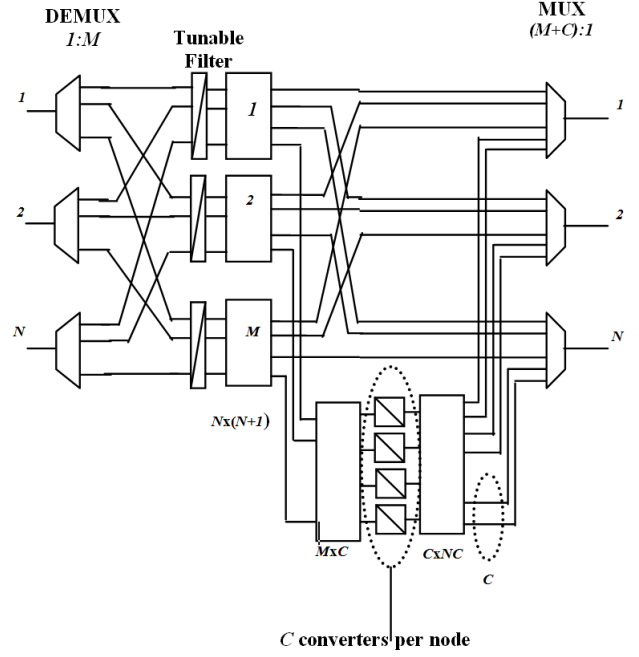


**Fig.2:** A Multistage Share-Per-Node Architecture of L-WIXC SSM (SSM-2).

wavelength number, a group of wavelength should be added. Though,  $S_G$  and  $G$  can be selected according to the demand but we have kept them limited such that  $C = S_G - 1$ ,  $G = \lceil M/S_G \rceil$  and  $G \in [2, N]$ . Here,  $C$  is the number of converters per *SSM* and  $C_T$  is the total number of converters such that,  $C_T = CM$  and  $M \leq C_T \leq NM$ . Anyway, those new wavelengths should form one of several groups which are not connected to other existing groups and do not affect the built structure. Note that, if  $N$  is larger than the size of group  $S_G$ , there will be more than one same fixed WCs in one group. It is some sort of redundancy. The *SSM* will have a total of  $2NM + (N + \lceil C_T/M \rceil)^2$  cross-points. Here, for instance and for simplification, we have kept the values of certain parameters like  $N$ ,  $M$ ,  $S_G$  and  $G$  fixed, as shown in Fig. 3 below

## 3. CALCULATION OF CROSSTALK

### 3.1 Single Stage L – WIXC, SSM-1

Assuming, the *SSM-1 L – WIXC* is fully loaded and each signal passing through the *L – WIXC* will be interfered by a total of  $2(M-1) + (N-1)M + C$  Homodyne Crosstalk contributions.  $(M-1)$  of which are leaked by the De-Multiplexer containing the main signal,  $(N-1)M$  are leaked by the other De-Multiplexers,  $C$  are leaked by the wavelength converter lines and other  $(M-1)$  are leaked at the Multiplexer containing the main signal.

Defining  $X_i$ , the number of contributions leaked from each  $i^{th}$  signal is random, and ranges from 0 to  $(M-1)$  in the first stage De-Multiplexer and other 0 to  $(M-1)$  in the last stage Multiplexer depending on

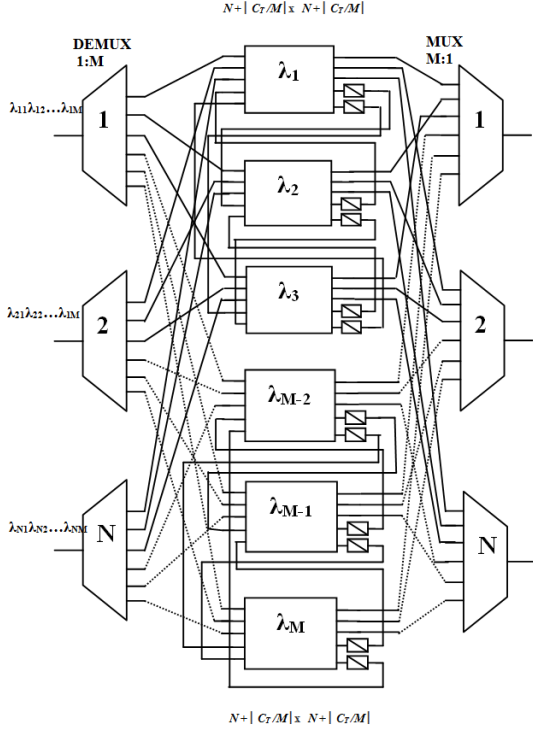


**Fig.3:** A Multistage Share-Per-Wavelength Grouped Architecture of  $L$ -WIXC(SSM-3) with Three SSM Per Group.

the cross-connecting state of the  $L$ -WIXC. Defining  $X_j$  ( $j = [2, N] \in [1, (N-1)M]$ ) as the number of contributions leaked from  $\lambda_{j1}$  in the same state of the OXC while taking into account the contributions leaked by the SSMs in the architectures. Finally, defining  $C$  as the number of contributions leaked from wavelength converters. So, the total crosstalk contribution in SSM-1 architecture is:

$$X1 = X_i + \sum_{j=2}^N X_j + C = 2(M-1) + (N-1)M + C \quad (1.1)$$

### 3.2 Multi-Stage $L$ -WIXC, SSM-2

Like SSM-1, in SSM-2 each signal will be interfered by a total of  $2(M-1) + (N-1) + C$  Homodyne Crosstalk contributions. Out of them,  $(M-1)$  of which are leaked by the De-Multiplexer containing the main signal,  $(N-1)$  are leaked by other De-Multiplexers,  $C$  are leaked by the wavelength converter lines and other  $(M-1)$  are leaked finally at the Multiplexer containing the main signal.

If  $X_i$  ( $i = [1, N] \in [0, M-1]$ ),  $X_j$  ( $j = [2, N] \in [1, M]$ ) and  $C$  bears their usual meaning, the total crosstalk contribution in SSM-2 architecture is:

$$X2 = X_i + \sum_{j=2}^N X_j + C = 2(M-1) + (N-1) + C \quad (1.2)$$

### 3.3 Grouped $L$ -WIXC, SSM-3

In SSM-3, each signal will be interfered by a total of  $(M-1) + M(N-1) + C[(M-1) + M(N-1) + N + C - 1]$  Homodyne Crosstalk contributions. Out of them  $(M-1)$  of which are leaked by the De-Multiplexer containing the main signal,  $M(N-1)$  are leaked by other De-Multiplexers. The rest of the portion is coming from and going to other  $C$  SSMs of a Group of size  $S_G$ . In each of the  $C$  (no. of wavelength converters per SSM) number of SSMs, signal from each converter line will interfere and will be interfered by  $N$  signals coming out from the SSMs and other  $(C-1)$  converter lines. Mentionable that, before entering in each of the  $C$  number of SSMs, each signal will be interfered by crosstalk contributions leaked by the other De-Multiplexers, those do not contain the main signal.

If  $X_i$  ( $i = [1, N] \in [0, M-1]$ ) and  $X_j$  ( $j = [2, N] \in [1, M]$ ) bears their usual meaning then,  $X_l$  ( $l = [1, C] \in (X_i, X_j$  and  $[1, N + C - 1]$ ) is defined as the total number of crosstalk contributions leaked due to the wavelength converter lines. Now, the total crosstalk contribution in SSM-3 architecture is:

$$X3 = X_i + \sum_{j=2}^N X_j + X_l = (M-1) + M(N-1) + C[(M-1) + M(N-1) + N + C - 1] \quad (1.3)$$

### 3.4 The Electric Field, $E(t)$

Now, considering both the SSM-1 and SSM-2 architectures, the general Electric Field of the main signal and all the crosstalk contributions can be expressed as [1]

$$\begin{aligned} |\vec{E}(t)| &= |\vec{E}| b_{mn}(t) \cos[\omega_{mn}(t) + \phi_{mn}(t)] \vec{P}_{mn} \\ &+ \sum_{\substack{i=1 \\ i \neq m}}^{i=M} \sqrt{\epsilon_i} |\vec{E}| b_{mn}(t - \tau_{in}) \cos[\omega_{mn}(t - \tau_{in}) + \phi_{mn}(t - \tau_{in})] \vec{P}_{in} \\ &+ \sum_{\substack{j=Ni=M \\ j=1 \\ j \neq n}}^{j=Ni=M} \sum_{i=1} \sqrt{\epsilon_{ij}} |\vec{E}| b_{mn}(t - \tau_{ij}) \cos[\omega_{mn}(t - \tau_{ij}) + \phi_{mn}(t - \tau_{ij})] \vec{P}_{ij} \\ &+ \sum_{\substack{l=C \\ l \neq m}}^{l=C} \sqrt{\epsilon_{il}} |\vec{E}| b_{mn}(t - \tau_{il}) \cos[\omega_{mn}(t - \tau_{il}) + \phi_{mn}(t - \tau_{il})] \vec{P}_{il} \end{aligned} \quad (2.1)$$

In contrast to that, the Electric Field of the main signal and all the crosstalk contributions of the SSM-3 can be expressed in (2.2)

$$\begin{aligned}
|\overrightarrow{E}(t)| &= |\overrightarrow{E}|b_{mn}(t)\cos[\omega_{mn}(t)+\phi_{mn}(t)]\overrightarrow{P}_{mn} \\
&+ \sum_{\substack{i=1 \\ i \neq m}}^{i=M} \sqrt{\epsilon_i} |\overrightarrow{E}|b_{mn}(t-\tau_{in})\cos[\omega_{mn}(t-\tau_{in})+\phi_{mn}(t-\tau_{in})]\overrightarrow{P}_{in} \\
&+ \sum_{\substack{j=1 \\ j \neq n}}^{j=N} \sum_{i=1}^{i=M} \sqrt{\epsilon_{ij}} |\overrightarrow{E}|b_{mn}(t-\tau_{ij})\cos[\omega_{mn}(t-\tau_{ij})+\phi_{mn}(t-\tau_{ij})]\overrightarrow{P}_{ij} \\
&+ \sum_{\substack{l=1 \\ l \neq m}}^{l=C} \sum_{\substack{p=1 \\ p \neq m}}^{p=N+C-1} \sqrt{\epsilon_{lp}} |\overrightarrow{E}|b_{mn}(t-\tau_{lp})\cos[\omega_{mn}(t-\tau_{lp})+\phi_{mn}(t-\tau_{lp})]\overrightarrow{P}_{lp} \\
&+ \sum_{\substack{i=1 \\ i \neq m}}^{i=M} \sqrt{\epsilon_{il}} |\overrightarrow{E}|b_{mn}(t-\tau_{il})\cos[\omega_{mn}(t-\tau_{il})+\phi_{mn}(t-\tau_{il})]\overrightarrow{P}_{il} \\
&+ \sum_{\substack{j=1 \\ j \neq n}}^{j=N} \sum_{i=1}^{i=M} \sqrt{\epsilon_{ij}} |\overrightarrow{E}|b_{mn}(t-\tau_{ij})\cos[\omega_{mn}(t-\tau_{ij})+\phi_{mn}(t-\tau_{ij})]\overrightarrow{P}_{ij}
\end{aligned} \tag{2.2}$$

Here,  $|E|$  is the signal amplitude which is assumed to be unchanged as the leaked power is considerably low;  $b_{mn}(t)$ ,  $b_{mn}(t-\tau_{in})$ ,  $b_{mn}(t-\tau_{ij})$ ,  $b_{mn}(t-\tau_{il})$  and  $b_{mn}(t-\tau_{lp})$  are the Binary Data Sequences with values of 0 or 1 in a bit period  $T$  of  $\lambda_{mn}$ ,  $\lambda_{in}$ ,  $\lambda_{ij}$ ,  $\lambda_{il}$  and  $\lambda_{lp}$  respectively. Now  $\omega_{mn}(t)$  and  $\Phi_{mn}(t)$ ,  $\omega_{mn}(t-\tau_{in})$  and  $\Phi_{mn}(t-\tau_{in})$ ,  $\omega_{mn}(t-\tau_{ij})$  and  $\Phi_{mn}(t-\tau_{ij})$ ,  $\omega_{mn}(t-\tau_{il})$  and  $\Phi_{mn}(t-\tau_{il})$  and  $\omega_{mn}(t-\tau_{lp})$  and  $\Phi_{mn}(t-\tau_{lp})$  are the Centre Frequencies and Phase Noises of the LASERS, respectively;  $\overrightarrow{P}_{mn}$ ,  $\overrightarrow{P}_{in}$ ,  $vecP_{ij}$ ,  $vecP_{il}$  and  $vecP_{lp}$  are the Time-invariant unit magnitude polarization vectors of the main signal and its crosstalk contributions, respectively;  $\tau_{in}$ ,  $\tau_{ij}$ ,  $\tau_{il}$  and  $\tau_{lp}$  are the Propagation Delay Differences of the contributions;  $\epsilon_i$ ,  $\epsilon_{ij}$ ,  $\epsilon_{lp}$ ,  $\epsilon_{il}$  are the Optical Power ratio of each crosstalk contribution to the signal. For simplification, we assume that, all the crosstalk contributions have the same power ratio. Here, the subscripts  $m$  and  $n$  are fixed values, correspond a signal generated from  $n^{th}$  De-Multiplexer and destined towards  $m^{th}$  SSM. Besides, the subscripts  $i$ ,  $j$ ,  $l$  and  $p$  are variables but bears the meaning the same way as  $m$  and  $n$ .

The first terms of the right part of (2.1) and (2.2) are the fields of the main signal and the second terms are the crosstalk contributions leaked from the main signal itself. The third and fourth terms are the contributions leaked by the signals from other SSMs having same wavelength and by the wavelength converter lines respectively. However the fourth term also corresponds to the contribution leaked by the wavelength converters from other SSMs of a group.

### 3.5 If $\tau(\tau_{in}, \tau_{ij}, \tau_{li} \text{ and } \tau_{lp}) > \tau_{coherent}$

If the optical propagation delay differences in an OXC exceed the coherent time of the LASER,  $\Phi_{mn}(t)$  is not correlated with  $\Phi_{mn}(t-\tau_{in})$ ,  $\Phi_{il}(t-\tau_{ij})$ ,  $\Phi_{mn}(t-\tau_{il})$  and  $\Phi_{mn}(t-\tau_{lp})$  are also not correlated with each other for different values of  $i, j, l$  and  $p$ . Therefore, all the crosstalk contributions, which are incoherent with each other, are also incoherent with the main signal. In this case, the generalized Electric Field of the main signal and all other crosstalk contributions in SSM-1, 2 and 3 can be expressed as [4]

$$\begin{aligned}
|\overrightarrow{E}(t)| &= |\overrightarrow{E}|b_{mn}(t)\cos[\omega_{mn}(t)+\phi_{mn}(t)]\overrightarrow{P}_{mn} \\
&+ \sum_{S=1}^{S=X_N} \sqrt{\epsilon_S} |\overrightarrow{E}|b_S(t)\cos[\omega_S(t)+\phi_S(t)]\overrightarrow{P}_S \\
&+ \sum_{r=1}^{r=X_E} \sqrt{\epsilon_r} |\overrightarrow{E}|b_r(t)\cos[\omega_r(t)+\phi_r(t)]\overrightarrow{P}_r
\end{aligned} \tag{3}$$

Where,  $b_s(t)$  and  $b_r(t)$ ,  $\omega_s(t)$  and  $\omega_r(t)$ ,  $\Phi_s(t)$  and  $\Phi_r(t)$  and  $\overrightarrow{P}_s$  and  $\overrightarrow{P}_r$  are the binary data sequences, centre frequencies, phase noises and unit magnitude polarization vectors of the  $s^{th}$  and  $r^{th}$  crosstalk contributions respectively. Here,  $b_s(t)$  and  $b_r(t)$  are not correlated with  $b_{mn}(t)$  even for the contributions leaked from the main signal itself because  $\tau$  is long enough and they are not synchronous. Besides, in (3)  $X_N$  denotes crosstalk contributions by the signals originated from other SSMs and by the signals originated by the main signal itself. In contrast to that,  $X_E$  denotes crosstalk contributions originated by wavelength converters. Assuming all the  $N$  signals with wavelength 1 have exact the same centre frequency, i.e.,  $\omega_{mn} = \omega_s = \omega_r$ , when  $b_{mn}(t) = 1$ . The normalized photocurrent caused by the signal and crosstalk in SSM-1, 2 and 3 are [3]

$$\begin{aligned}
|\overrightarrow{I}(t)| &= 1+2\sqrt{\epsilon} [ \sum_{p=1}^{S=X_N} b_p(t)\cos[\phi_{mn}(t)+\phi_s(t)]\overrightarrow{P}_{mn} \cdot \overrightarrow{P}_s \\
&+ \sum_{S=1}^{S=X_E} b_l(t)\cos[\phi_{mn}(t)+\phi_r(t)]\overrightarrow{P}_{mn} \cdot \overrightarrow{P}_r \\
&+ \sum_{q=1}^{q=X_N+X_E} b_{sr}(t)\cos[\phi_s(t)+\phi_r(t)]\overrightarrow{P}_S \cdot \overrightarrow{P}_r
\end{aligned} \tag{4}$$

The second and third term in the right part of (4) are the signal-crosstalk beat noises and are results of the LASERS *Relative Intensity Noise* (RIN). The terms of high orders of are neglected because  $\epsilon$  is considerably low. By calculating the *Auto Co-variance* of

the beat noise and making *Fourier Transformation*, the noise powers of *SSM-1* can be expressed as:

$$\sigma^2_{RIN} = \varepsilon \left[ \sum_{S=1}^{S=X_N} \cos^2 \theta_s + \sum_{r=1}^{r=X_E} \cos^2 \theta_r + \sum_{q=1}^{q=X_E+X_N} \cos^2 \theta_{sr} \right] \quad (5)$$

Where,  $\cos^2 \theta_s = \frac{\vec{P}_{mn} \cdot \vec{P}_s}{|\vec{P}_{mn}| |\vec{P}_s|}$ ,  $\cos^2 \theta_r = \frac{\vec{P}_{mn} \cdot \vec{P}_r}{|\vec{P}_{mn}| |\vec{P}_r|}$  and  $\cos^2 \theta_{sr} = \frac{\vec{P}_{mn} \cdot \vec{P}_s}{|\vec{P}_{mn}| |\vec{P}_s|}$ .

Here,  $\theta_s$ ,  $\theta_r$  and  $\theta_{sr}$  are the polarization angles difference between the crosstalk contributions and the signal. Assuming both the beat noise and receiver noise have Gaussian probability density distribution, the *BitErrorRate* (*BER*) for  $\tau > \tau_{coherent}$  can be expressed as:

$$BER_{SSM} = \frac{1}{4} \operatorname{erfc} \left[ \frac{I_{SSM} - I_D}{\sqrt{2} \sqrt{\sigma_o^2 + \sigma_{RIN}^2 + \sigma_X^2 + \sigma_{oth}^2}} \right] + \frac{1}{4} \operatorname{erfc} \left[ \frac{I_D}{\sqrt{2} \sigma_o} \right] \quad (6)$$

Where,  $\sigma_o^2$  denotes the receiver noise i.e. *ThermalNoise* and *ShotNoise* which exist in the absence of crosstalk;  $\sigma_X^2$  denotes the Crosstalk Power which is equal to  $R_d P_{in} \alpha^2 N_x$ ;  $\sigma_{RIN}^2$  denotes the Relative Intensity Noise power and  $\sigma_{oth}^2$  denotes the other types of noise i.e. signal to spontaneous noise and spontaneous to spontaneous noise which are actually negligible. Here,  $R_d$  is the Responsivity,  $P_{in}$  is the input power,  $\alpha$  is the power ratio and  $N_x$  is the number of cross points in the *SSM*. For a fixed value of decision threshold setting,  $I_D = 0.5 I_{SSM}$  the expression for power penalty can be written as [6]

$$pp(dB) = -5 \log_{10} \left( 1 - \frac{4 \sigma_{RIN}^2 Q^2}{I_{SSM}^2} \right) \quad (7)$$

In the worst case scenario, for the maximum value of noise power [3], the expression of maximum power penalty of *SSM-1*, *SSM-2* and *SSM-3* when the products of Cosine components are either +1 or -1 are given below:

$$Max^m pp_{SSM-1}(dB) = -5 \log_{10} [1 - 4 \in (2(M-1) + (N-1)M + C)Q^2] \quad (8.1)$$

$$Max^m pp_{SSM-2}(dB) = -5 \log_{10} [1 - 4 \in (2(M-1) + (N-1) + C)Q^2] \quad (8.2)$$

$$Max^m pp_{SSM-3}(dB) = -5 \log_{10} [1 - 4 \in ((C+1)(MN-1) + C(N+C-1))Q^2] \quad (8.3)$$

In the above discussion  $BER_{SSM}$ ,  $I_{SSM}$  and  $\sigma_{RIN}^2$  can be replaced by either  $BER_{SSM-1}$ ,  $I_{SSM-1}$  and  $\sigma_{RIN,SSM-1}^2$  or  $BER_{SSM-2}$ ,  $I_{SSM-2}$  and  $\sigma_{RIN,SSM-2}^2$  or  $BER_{SSM-3}$ ,  $I_{SSM-3}$  and  $\sigma_{RIN,SSM-3}^2$ .

## 4. RESULTS AND DISCUSSIONS

The results and overall performance are evaluated in terms of Bit Error Rate (*BER*) and Power Penalty (*pp*) following the analytical approach presented in sec. 3 for three *L-WIXC* architectures i.e. *SSM-1*, *SSM-2* and *SSM-3*. The following parameters are kept fixed for convenient numerical computations. They are: crosstalk power ratio,  $\alpha = -30$  dB and  $Q = 6$  for a  $BER = 10^{-9}$ . For both cases, the number of input wavelengths ( $W$ ) per input channel ( $N$ ) is assumed to be equal to the total number of *SSMs* ( $M$ ) needed in the architectures. The total number of Wavelengths Converters ( $C$ ) is varied according to the limiting condition mentioned earlier.

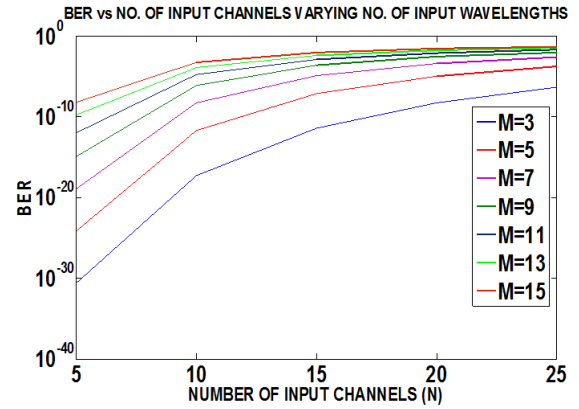


**Fig.4:** *BER vs. Number of Input Channels (N) Varying Number of Input Wavelengths (M) for SSM-1.*

Fig. 4, 5 and Fig. 6 are the plots of *BER* vs. Number of Input Channels ( $N$ ) varying the number of Input Wavelengths or number of *SSMs* ( $M$ ) for single stage, multistage Share-per-Node and multistage Share-per-Wavelength grouped architectures respectively. The plots above illustrates that, for a particular value of  $M$ , *BER* increases with the increase of number of Input Channels ( $N$ ), while the number of *SSMs* ( $M$ ) and Number of input wavelengths ( $W$ ) per input channel are assumed to be equal. It can also be shown from the plots that, at lower values of  $N$ , single stage and multi-stage *L-WIXC*s experience more *BER* than grouped Share-per-Wavelength

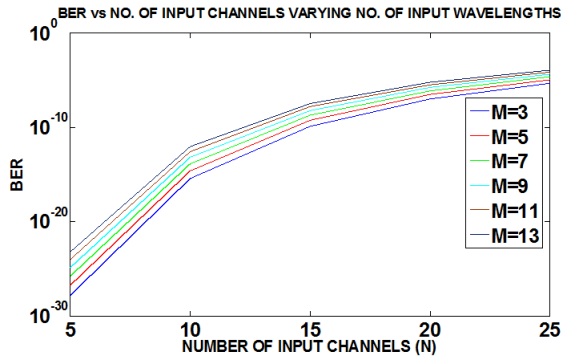


**Fig. 5:** BER vs. Number of Input Channels ( $N$ ) Varying Number of Input Wavelengths ( $M$ ) for SSM-2.

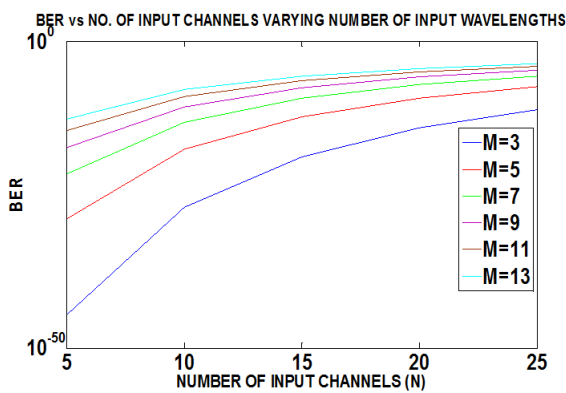


**Fig. 6:** BER vs. Number of Input Channels ( $N$ ) Varying Number of Input Wavelengths ( $M$ ) for SSM-3.

$L - WIXC$  for a fixed value of  $M$ .  $BER$  also increases for higher values of  $M$  while parameters like Input Power ( $pin - dBm$ ), Component Crosstalk ( $\epsilon$ ) and Number of converters ( $C$ ) are kept fixed at  $-20$  dBm,  $-60$  dBm and  $12$  dBm respectively.

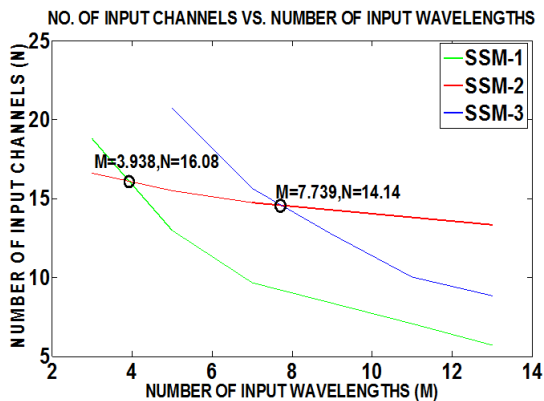


**Fig. 7:** No. of Input Channels ( $N$ ) vs. Number of Input Wavelengths ( $M$ ) for SSM-1, SSM-2 and SSM-3.

Fig. 7 is a plot of number of Input Channels ( $N$ ) vs. number of input wavelengths per input channel ( $M$ ) which is derived from the plots of  $BER$  vs.  $N$  varying  $M$  for a fixed value of  $BER = 10^{-9}$  in Fig. 4, 5 and 6. It also shows that,  $N$  decreases with the increase of  $M$ . As the number of Input Channels ( $N$ ) and number of Input Wavelengths ( $M$ ) should be discrete integers, the cross points shown in the fig. 07 should be rounded off to  $(M, N) \equiv (4, 17)$  and  $(M, N) \equiv (8, 15)$ . For a particular value of number of Input Wavelengths,  $M < 4$ , SSM-2 (multi-stage  $L - WIXC$ ) needs less number of Input Channels,  $N$  (both in Multiplexer & De-multiplexer) compared to other two architectures for maintaining a fixed performance at  $BER = 10^{-9}$ . SSM-2 gives better performance compared to SSM-3 (Share-per-Wavelength  $L - WIXC$ ) in terms of number of input channels ( $N$ ) for the values of  $M$ , around  $4 < M < 8$  and outside this range its performance degrades than the other two architectures. So, SSM-1 (single-stage  $L - WIXC$ ) and SSM-3 (Share-Per-Wavelength  $L - WIXC$ ) can support more number of input wavelengths than SSM-2 (multistage  $L - WIXC$ ), providing less number of input channels which reduces the cost and complexity of the network. Up to the range of analytical calculation given here, it is obvious that, SSM-1 is the best among the three architectures.

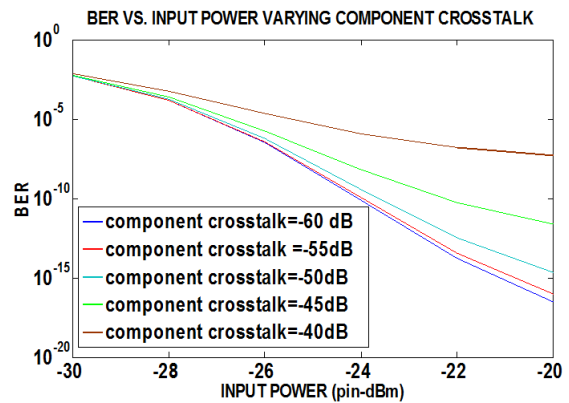


**Fig. 8:** BER vs. Input Power ( $pin - dBm$ ) Varying Component Crosstalk for SSM-1.

Fig. 8, 9 and 10 are the plots of  $BER$  vs. Input Power ( $pin - dBm$ ) varying the Component Crosstalk ( $\epsilon$ ) for a given value of number of input wavelengths,  $M = 5$ , number of input channels,  $N = 10$  and number of converters,  $C = 4$ . It also shows that,  $BER$  increases with the increase of Component Crosstalk ( $\epsilon$ ). From the figures, we can also calculate the Power Penalties ( $pp$ ) at a fixed  $BER = 10^{-9}$  for different values of  $\epsilon$ .

Fig. 11 is a plot of Power Penalty ( $pp$ ) vs. Component Crosstalk ( $\epsilon$ ) comparing the three architectures i.e. SSM-1, SSM-2 and SSM-3, which is derived from the plots of  $BER$  vs. Input Power ( $pin - dBm$ )

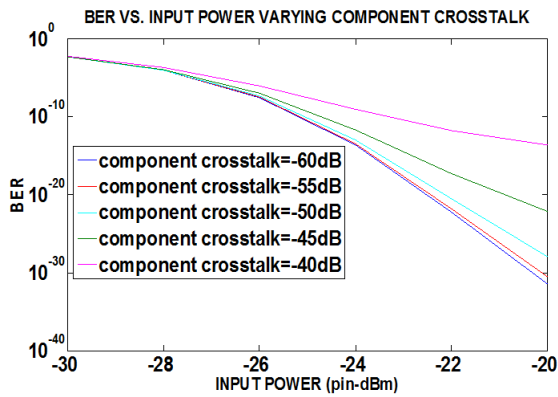


Fig. 9: BER vs. Input Power (pin-dBm) Varying Component Crosstalk for SSM-2.

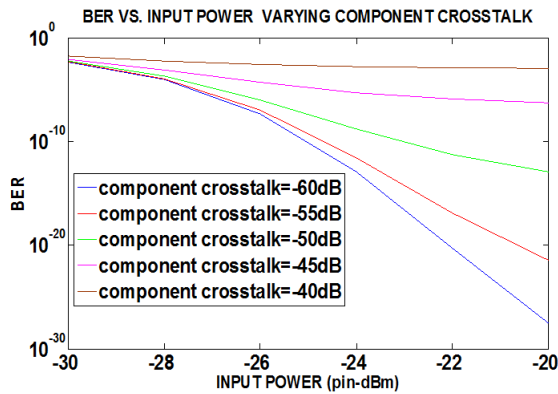


Fig. 10: BER vs. Input Power (pin-dBm) Varying Component Crosstalk for SSM-3.

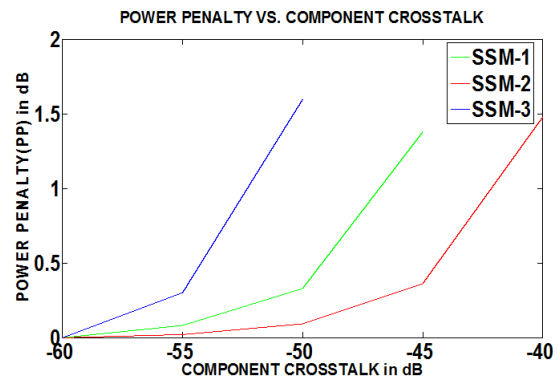


Fig. 11: Power Penalty (pp) vs. Component Crosstalk ( $\epsilon$ ) for SSM-1, SSM-2 and SSM-3 from Analytical Data.

varying  $\epsilon$  for a fixed value of  $BER = 10^{-9}$  in Fig. 8,9 and 10. The figure also illustrates that, up to -55 dB of Component Crosstalk ( $\epsilon$ ), Power Penalties (pp) are almost similar for all the architectures. After that, Power Penalty (pp) of SSM-3 (Share-Per-Wavelength  $L - WIXC$ ) increases more rapidly compared to SSM-1 and SSM-2 with the increase of  $\epsilon$ . Moreover, it also unveils that, SSM-1 has the least Power Penalty (pp) among them.

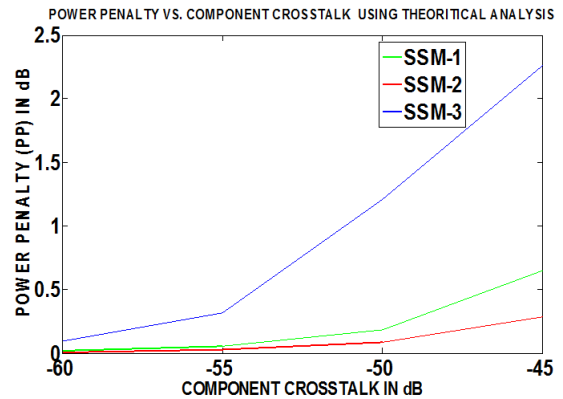


Fig. 12: Power Penalty (pp) vs. Component Crosstalk ( $\epsilon$ ) for SSM-1 and SSM-2 from Theoretical Data.

Fig. 12 is a plot between Power Penalty (pp) and Component Crosstalk ( $\epsilon$ ) illustrating the theoretical comparison among SSM-1, SSM-2 and SSM-3. The plot is derived from (8.1), (8.2) and (8.3). This figure is also derived for the given values of Number of Input Channels,  $N = 10$ , number of Input Wavelengths,  $M = 5$  and Number of Converters,  $C = 4$ . Like Fig. 11, this figure gives almost the same result i.e. up to -55 dB of Component Crosstalk ( $\epsilon$ ) all the architectures have almost same Power Penalties (pp) and after that, Power Penalty (pp) of SSM-3 increases more rapidly compared to SSM-1 and SSM-2.

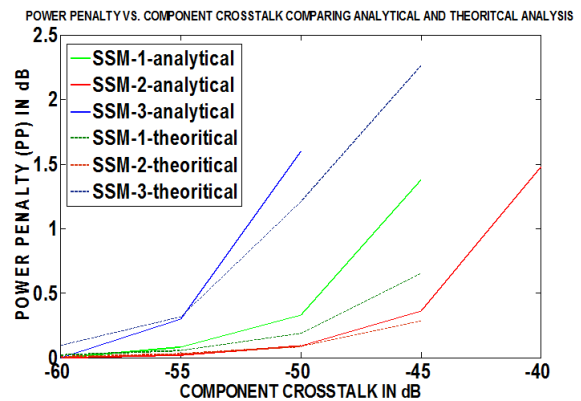


Fig. 13: Power Penalty (pp) vs. Component Crosstalk ( $\epsilon$ ) for SSM-1 & SSM-2 from Analytical & Theoretical Data.

Fig. 13 shows the comparison between the analytical and theoretical values of Power Penalty ( $pp$ ) and Component Crosstalk ( $\varepsilon$ ) for  $SSM-1$ ,  $SSM-2$  and  $SSM-3$ . As per analysis, there are little differences between analytical and theoretical values of Power Penalty ( $pp$ ) for each  $SSM$ . This plot also shows that,  $SSM-3$  suffers from more Power Penalty ( $pp$ ) compared to  $SSM-1$  and  $SSM-2$  in both theoretical and analytical approach.

## 5. CONCLUSION

The Crosstalk contributions in three different  $L - WIXC$  architectures (a single stage Share-Per-Node, a multistage Share-Per-Node and a multistage grouped Share-Per-Wavelength  $L - WIXC$ ) are identified and three models are presented to quantify the impact of both Coherent and Incoherent Crosstalk contribution from different sources and due to different delay differences. It was found that, Crosstalk increases with the increase of the Number of Input wavelengths ( $M$ ) and the Number of Input Channels ( $N$ ) due the Leakage Crosstalk Contributions from each stage in all the architectures. Moreover, it can be said that, for a fixed value of Component Crosstalk ( $\varepsilon$ ),  $SSM - 3$  suffers more from Crosstalk compared to  $SSM - 1$  and  $SSM - 2$ . In designing a more practical architecture and accurately analyse a  $L - WIXC$  Share-Per-Node architecture, the Crosstalk Power due to the Total Number of Cross-points should be considered and there-by parameters like  $N$  and  $M$  should be chosen in a way to get optimum performance i.e. minimum  $BER$  and Power Penalty ( $pp$ ). Under regular circumstances i.e. when the Number of Input Wavelengths ( $M$ ) are within a optimum level and there are greater Number of Input Channels ( $N$ ) available, a multistage  $L - WIXC$  architecture (e.g.  $SSM - 2$ ) is a formidable candidate compared to its single-stage Share-Per-Node and Share-Per-Wavelength counterparts in designing a optical network with reduced impact of crosstalk as well as cost. In contrast to that, if the network has limited number of Input Channels, the single stage architectures are preferred because they allow more wavelengths per channel. In contrast to that, it is shown that, proper utilization of grouped Share-Per-Wavelength architecture greatly improves the Blocking Performance of a network [6]. In this paper, performance of single stage Share-Per-Node, multi-stage Share-Per-Node and multistage grouped Share-Per-Wavelength architectures are analytically evaluated and their performances are compared with respect to Coherent and Incoherent Crosstalk from different sources. Finally, it can be concluded that, in spite of having less Blocking Probability [6], the grouped  $L - WIXC$  faces more Power Penalty ( $pp$ ) and can support less Input Wavelengths up to a certain level of Input and less Number of Wavelength Converters when compared to the ungrouped single-stage Share-

Per-Node architecture. In contrast to that, under same circumstances, Share-Per-Wavelength architecture is better than the multi-stage  $L - WIXC$  architecture ( $SSM - 2$ ).

## References

- [1] T.Y.Chai, T.H.Cheng, S.K.Bose, C.Lu and G.Shen, "Crosstalk Analysis for Limited-Wavelength-Interchanging Cross Connects," *IEEE Photon. Technol. Lett.*, vol. 14, pp. 696–698, May 2002.
- [2] F. Yan, W. Hu, W. Sun, W. Guo and Y. Jin, "Efficient Sharing of Fixed Wavelength Converters in Clos-Type Wavelength Interchanging Cross Connects," *J. Lightwave Technol.*, vol. 27, no. 19, October 1, 2009.
- [3] H. Takahashi, K. Oda, and H. Toba, "Impact of crosstalk in an arrayed waveguide multiplexer on  $N \times N$  optical interconnection," *J. Lightwave Technol.*, vol. 14, pp. 1097–1105, June 1996.
- [4] Y. Shen, K. Lu, and W. Gu, "Coherent and incoherent crosstalk in WDM optical networks," *J. Lightwave Technol.*, vol. 17, pp. 759–764, May 1999.
- [5] T.Y.Chai, T.H.Cheng, G.Shen, S.K.Bose and C.Lu, "Design and Performance of Optical Cross-Connect Architectures with Converter Sharing," *O. Networks Magazine*, pp. 73–84, July/August 2002.
- [6] P. Hu, Y. Wang and W. Hu, "A new grouped limited-wavelength-conversion optical cross-connect and its scalability performance," *Optical Transmission, Switching, and Subsystems II*, Proc. Of SPIE Vol. 5625.
- [7] S. Sarkar, N. R. Das, "Study of Component Crosstalk and Obtaining Optimum Detection Threshold for Minimum Bit-Error-Rate in a WDM Receiver," *J. Lightwave Technol.*, vol. 27, no. 19, October 1, 2009.
- [8] M.R. Karim, S.P. Majumder, "Analysis of ASE and intraband crosstalk limitations in FBG-OC-Based bidirectional optical cross connects in a WDM ring network," *International Journal of Electronics, Computer & Communications Technologies*, vol. 2(2), 2012.



**Md Asif Iqbal** obtained his Bachelor of Science degree in Electrical, Electronic and Communication Engineering (EECE) in 2010 from Military Institute of Science and Technology (MIST), Bangladesh which is affiliated to Bangladesh University of Professionals (BUP). He is continuing his M.Sc. degree in the department of Electrical and Electronic Engineering (EEE) at Bangladesh University of Engineering and Technology (BUET), Bangladesh. He is currently working as a lecturer in the department of EECE in MIST since

January 2010. His research interests include Optical Cross-Connect Networks, Optical Network Design and Photonics.



**Mohammad Manzoor-E-Elahee** obtained his Bachelor of Science degree in Electrical, Electronic and Communication Engineering in 2010 from Military Institute of Science and Technology (MIST), Bangladesh which is affiliated to Bangladesh University of Professionals. He is currently working as an Assistant Officer Grade-1 (Networking) at Information & Communication Technology Division, Islami Bank Bangladesh

Limited (IBBL). His field of interests include Optical Cross-Connect Networks and Network and Routing Algorithm.



**Satya Prasad Majumder** is currently working as a DEAN and professor in the department of Electrical and Electronic Engineering (EEE) in Bangladesh University of Engineering and Technology (BUET). He is an active researcher in the field of communication and he has a number of publications in reputed international journals and conference proceedings. His fields of interests include Optoelectronics and Photonics, Optical

Switching Networks and Wireless Communications.